Published in final edited form as:
*J Am Chem Soc*. 2009 April 15; 131(14): 5313–5320. doi:10.1021/ja900067c.

# The Effects of NHC-Backbone Substitution on Efficiency in Ruthenium-based Olefin Metathesis

**Kevin M. Kuhn**, **Jean-Baptiste Bourg**, **Cheol K. Chung**, **Scott C. Virgil**[†], and **Robert H. Grubbs**[*]

Contribution from the Arnold and Mabel Beckman Laboratory of Chemical Synthesis, Division of Chemistry and Chemical Engineering, California Institute of Technology, Pasadena, California 91125.

## Abstract

A series of ruthenium olefin metathesis catalysts bearing N-heterocyclic carbene (NHC) ligands with varying degrees of backbone and *N*-aryl substitution have been prepared. These complexes show greater resistance to decomposition through C–H activation of the *N*-aryl group, resulting in increased catalyst lifetimes. This work has utilized robotic technology to examine the activity and stability of each catalyst in metathesis, providing insights into the relationship between ligand architecture and enhanced efficiency. The development of this robotic methodology has also shown that, under optimized conditions, catalyst loadings as low as 25 ppm can lead to 100% conversion in the ring-closing metathesis of diethyl diallylmalonate.

## Introduction

Olefin metathesis has emerged as a valuable tool in both organic and polymer chemistry.[1] Ruthenium-based catalysts, in particular, have received considerable attention because of their tolerance to moisture, oxygen, and a large number of organic functional groups.[2] Following the report of the increased activity of complex **1** ($H_2$IMes)($PCy_3$)$Cl_2$Ru=CHPh ($H_2$IMes = 1,3-dimesitylimidazolidine-2-ylidene),[3] and Hoveyda's subsequent exchange of the phosphine ligand with a chelating ether moiety (**2**),[4] many researchers have focused on increasing catalytic activity, selectivity and stability through modification of the N-heterocyclic carbene (NHC) ligand.[5]

As ligand modification has led to improved catalyst activity, a variety of applications have become possible, including ring-closing metathesis (RCM), cross metathesis (CM), ring-opening cross metathesis (ROCM), acyclic diene metathesis polymerization (ADMET), and ring-opening metathesis polymerization (ROMP). Among those metathesis reactions, ring-closing metathesis has become the most commonly employed metathesis reaction in organic synthesis.[6] For this transformation, NHC catalysts, such as **1**, **2**, and more recently **3**, have allowed both high activity and increased catalyst lifetime to be realized (Chart 1).[3,4,5c]

Despite these advances, still more efficient catalysts are sought to increase the applicability of RCM in industry. In many cases, olefin metathesis is still plagued by catalyst deactivation and the requirement of high catalyst loadings.[6] Furthermore, decomposition products of olefin metathesis catalysts have been shown to be responsible for unwanted side reactions such as

E-mail: rhg@caltech.edu.
Efficiency in Olefin Metathesis
[†]Caltech Center for Catalysis and Chemical Synthesis.

olefin isomerization.[7] Increased catalyst loading could also potentially increase the level of residual ruthenium impurities in the final products, which becomes especially critical where reaction products are intended for pharmaceutical use.[8] Collectively, these issues have a direct influence on the operational cost of metathesis transformations. With these factors in mind, the next challenge in RCM is to substantially decrease the catalyst loading, thereby reducing both reaction cost and the challenges in product purification. To this effect, our goal has been to increase catalyst efficiency by developing even more stable and robust catalysts that still retain a high catalytic activity.

Recently, studies by our group and others have unveiled the decomposition pathways at play during metathesis reactions.[9] Among other degradation products, complexes derived from C–H activation of *N*-aryl substituents were reported. Since the NHC ring and the aryl substituent must approach co-planarity for C–H activation, it was anticipated that decomposition via C–H activation processes might be slowed by restriction of *N*-aryl group of the NHC ligand, and this might be achieved by placing sterically hindered groups on the NHC backbone. This hypothesis was confirmed by successfully preparing *N*-phenyl complexes **4** and **5** that are more resistant to the decomposition initiated by C–H activation (Chart 2).[5a,b] Having unsubstituted *N*-phenyl groups, these complexes display good and exceptional reactivity, respectively, in the formation of highly substituted olefins. Despite these improvements, complexes **4** and **5** are more prone to decomposition than **1** and **2**.[10]

To address and further understand the balance between activity and stability of **5**, we sought to investigate a homologous series of ruthenium catalysts bearing NHCs with varying degrees of backbone and aryl substitution. Molecular modeling and the calculations of Jensen et al. suggest that a catalyst bearing an NHC with mesityl groups at nitrogen and a fully methylated backbone would be an improvement over existing catalysts.[11] We expected that the degree of substitution could be central to increased activity and catalyst lifetimes.

Herein, we report the preparation and characterization of a series of catalysts bearing NHCs with varying degrees of backbone and aryl substitution. Initial evaluation of their performance in olefin metathesis demonstrated that the common assays were not effective at measuring the relative efficiencies of these catalysts at standard catalyst loadings.[12] While the standard conditions are excellent in evaluating the activity of new catalysts, they are not sensitive to small variations in the efficiency profile accompanying subtle modification in catalyst architecture.

In order to examine these small changes, we have developed a highly sensitive ppm level assay utilizing the precision and consistency of Symyx robotic technology. We utilized these techniques to examine the activity and stability of these catalysts in RCM at low catalyst loadings, providing increased insight into the relationship between ligand architecture and catalyst efficiency. The development of this methodology has also shown that, under optimized conditions, complete conversion in the RCM of diethyl diallylmalonate is observed with catalyst loadings as low as 25 ppm (0.0025 mol%).

## Results and Discussion

### Catalyst Syntheses

The preparation of the 1,1'-dimethyl- and 1,2-dimethyl-substituted imidazolinium chlorides **6** and **7** (Chart 3) have been previously reported by Bertrand and Çetinkaya, respectively.[13] Under analogous experimental conditions, imidazolinium chlorides **9** and **10**, featuring 2-methylphenyl (*o*-tolyl) groups were obtained in good yields. Unfortunately, separation of the *syn*- and *anti*- isomers of **10** proved to be extremely difficult, requiring the mixture to be carried forward.

Following the procedures previously reported by our group to access the NHC of complex **5**, we then attempted the preparation of the highly substituted imidazolinium salts bearing four methyl substituents.[5a] While imidazolinium chloride **11** was prepared without incident, we were unable to synthesize the intermediate tetramethylated diamine **13** of the corresponding *N*-mesityl analogue under various conditions (Scheme 1). Considering the trimethylated NHC to be sufficiently encumbered to prevent *N*-aryl rotation, we prepared **8** instead by Grignard addition followed by reduction and imidazolinium salt formation.

With precursors **6–11** in hand, the corresponding free carbenes were generated by treatment of the imidazolinium salts with potassium hexamethyldisilazide (KHMDS) at room temperature (Figure 1). These carbenes (prepared in situ) were reacted with commercially available $(PCy_3)RuCl_2{=}CH(o\text{-}OiPrC_6H_4)$ at 70 °C, affording the phosphine-free chelating ether complexes **15–20**. These complexes were isolated as crystalline green solids after flash column chromatography, and as solids are both air-and moisture-stable under standard conditions.

## Structural Analyses

To probe the electronic and steric effects of backbone substitution, crystals of **17** and **20** were grown and their molecular structures were confirmed by single-crystal X-ray crystallographic analysis (Figure 2). The complexes exhibit a distorted square pyramidal geometry with the benzylidene moiety occupying the apical position. When compared with its unsubstituted analogue **2**, the backbone substitution of **17** results in significant differences in three key structural parameters summarized in Table 1: (1) Ru-C(1) bond length, (2) C(1)-Ru-C(25) bond angle, and (3) the C(3)-N2-C(16) bond angle. Surprisingly, there are no major differences between the solid-state structures of complexes **3** and **20**.

The crystal structure of complex **17** suggests that the backbone methyl substituents push the *N*-mesityl groups toward the ruthenium center and as a result the NHC-Ru-benzylidene bond angle is also increased. However, the bond distance between the NHC carbene carbon and the Ru center is shorter in **17** (1.968 Å) than in **2** (1.980 Å). This effect can be explained by noting that the backbone methyl substituents increase the electron-donating ability of the NHC ligand. This effect is also seen in the IR carbonyl stretching frequencies of the *cis*-$[RhCl(CO)_2(NHC)]$ complexes **21–23** (Chart 4), where increased substitution resulted in lower frequencies.[14] These structural differences should have a significant impact on the efficiency of the different catalysts.

## Ring-Closing Metathesis (RCM) Activity

RCM is widely used in organic synthesis and serves as a standard assay to evaluate the relative efficiency of most ruthenium-based catalysts.[6,12] With this in mind, we began our metathesis activity studies by focusing on the catalytic activity of the *N*-mesityl series (**2**, **15–17**) in the RCM of diethyl diallylmalonate **24** to cycloalkene **25**. The reactions, utilizing 1 mol% catalyst in $CD_2Cl_2$ at 30 °C, were monitored by $^1H$ NMR spectroscopy (Figure 3). Interestingly, the plots of cycloalkene **25** concentration vs. time (Figure 3) revealed that the complexes effect the cyclization of **24**, but with slower reaction rates as backbone substitution is increased. The same trend was observed for the cyclization of diethyl allylmethallylmalonate **26** to form trisubstituted cyclic olefin **27**. However, in the very challenging RCM of diethyl dimethallylmalonate **28**, using 5 mol% catalyst in $C_6D_6$ at 60 °C, increased substitution resulted in increased catalyst lifetimes and higher conversions to tetrasubstituted cyclic olefin **29**.

Several explanations could exist to explain these contradictory results. Along with decreased initiation rate, increased backbone substitution could also alter propagation rate, stability, or a combination of both. In any case, the results indicate that the assays reported by Ritter, *et al.*,

while useful for evaluating the activity of new catalysts,[12] do not distinguish between catalysts that are both highly active[15] and stable.[16] Future improvements in, and understanding of, olefin metathesis catalysts will require a more sensitive assay to evaluate small variations in the efficiency profile accompanying subtle modification in catalyst architecture.

## Development of a ppm Level Assay

In order to study subtle differences in activity and stability, the standard RCM reactions should be observed at the lower limit of productive catalyst loading and under optimized conditions. With this in mind, new techniques were developed using a Symyx robotic system to maintain a high degree of precision and consistency when working with ultra-low catalyst loadings. Our group has recently used these robotic systems to optimize reaction conditions and investigate new applications in olefin metathesis.[17] Similarly, utilizing an automated Vantage system, Grela *et al.* recently reported the successful RCM of **24** at just 0.02 mol% **2**.[18]

A robotic assay was developed utilizing the RCM of diene **24** by complex **2**. Stock solutions of catalyst and substrate were prepared in a nitrogen-filled glovebox. While substrate stock solutions could be stored in septum-topped vials, catalyst solutions were prepared immediately prior to use. The Symyx core module was utilized to add all solutions to reaction vessels as well as to sample the reaction mixtures at programmed time intervals. Aliquots were added into ethyl vinyl ether solution at −20 °C,[19] and then analyzed by gas chromatography with dodecane as an internal standard, measuring the change in the amounts of substrate and product with time. With minimal deviation in reaction results, 1 M (1 mL vials) and 0.1 M (20 mL vials) concentrations were employed depending on reaction scale and glassware to minimize substrate usage. The large vials were used in experiments where aliquots were withdrawn over the course of the reaction.

For practical reasons, most standard metathesis assays are performed in a closed system under inert atmosphere.[12,18] However, we have observed variations in reaction rate and total conversion depending on the headspace of the reaction vessel. To circumvent this problem, reactions were carried out in open vials. Additionally, in order to minimize the potential for decomposition pathways related to oxygen, all reactions were conducted in a nitrogen-filled glovebox. While ruthenium-based catalysts are relatively stable under ambient conditions, at low catalyst loadings oxygen related decomposition becomes relevant. Control reactions were completed on a Symyx core module open to atmosphere, confirming the importance for oxygen-free reaction conditions (Figure 4).

Other reaction considerations, including temperature and solvent, were optimized based on our recent complementary studies on the RCM of diallylamines with low catalyst loadings.[17a] A solvent screen identified toluene as the optimal solvent for RCM of these diallyl substrates (Figure 4). Toluene as solvent also allowed for an increased temperature of 50 °C. While increased temperatures have previously been shown to increase metathesis reaction rates,[18, 20] temperatures above 50 °C decreased assay consistency and resulted in significant solvent losses throughout the course of the reaction. The use of methylene chloride, the solvent most commonly used for RCM, resulted in considerable solvent loss even at 30 °C. Furthermore, its use resulted in decreased conversions, relative to other solvents. The RCM of **24** was then monitored over a variety of catalyst loadings to calibrate the new assay (Figure 5). Under optimized conditions (0.1 M, toluene, 50 °C), complex **2** afforded almost quantitative yields of **25** after 1 hour at just 50 ppm.

Under the optimized conditions, trimethylated complex **17** required only 25 ppm to reach full conversion to disubstituted cycloalkene **25**; a catalyst loading near pharmaceutical impurity limits.[8] In order to directly compare the *N*-mesityl series (**2** and **15–17**), catalyst loadings were further decreased to 15 ppm to ensure that no reactions would reach completion before the

catalyst had completely decomposed. Again, at very low catalyst loadings, increased backbone substitution resulted in higher conversions to cyclic olefin **25**. When conversions were monitored over the course of the reaction, the effects of backbone substitution became evident (Figure 6a). The data suggest that the higher conversions are a direct result of longer catalyst lifetimes. However, as observed during the NMR studies, increased backbone substitution decreases catalyst reaction rate. These results were supported through observation of the same trends when complexes **3** and **20** were studied using the same assay (Figure 6b).[21]

The catalyst efficiency assay was then expanded to study the RCM of **26** to give trisubstituted cycloalkene **27**. Calibration using the more sterically challenging substrate revealed that significantly more catalyst is necessary to effect full conversion to **27**, with complex **2** affording yields over 90% at 400 ppm catalyst loadings (Figure 7). The increase in required catalyst loading due to the addition of a single methyl group demonstrates the importance and effect of the olefin substrates steric environment.

Catalyst comparison reactions, performed at 200 ppm, reveal that the addition of substituents to the NHC ligands has greater impact on the efficiency of the metathesis catalysts than with the previous substrate, with **17** and **20** both outperforming their unsubstituted analogues (Figure 8). Notably, the RCM of **26** also clearly highlights the difference in stability between the *N*-mesityl (**2** and **17**) and the *N*-*o*-tolyl catalysts (**3** and **20**). For this trisubstituted olefin substrate, catalyst stability is more significant than activity for success in RCM. Complex **5** is the most active ruthenium-based catalyst to date, but not particularly stable under prolonged reaction conditions. As expected, while **5** performs exceptionally well at standard loadings (1 mol%), it falters at low catalyst loadings.

Finally, the ring-closing metathesis of **28** to tetrasubstituted cycloalkene **29** was examined using the same catalyst assay. Continuing the trend, at 0.2 mol% loading, complex **17** outperforms **2**, yielding just 15% and 7% of the tetrasubstituted cycloalkene respectively (Figure 9). Despite the expected low yields, the result reaffirmed the conclusion that backbone substitution increases the stability of the resulting complex. In the case of the *N*-mesityl series, this increase in stability has not resulted in a detrimental decrease in activity.

Surprisingly, the *N*-*o*-tolyl series does not continue in the expected trend. Complexes **3**, and **20** were compared at 0.2 mol% catalyst loading (Figure 10), revealing complex **3** to be the most efficient catalyst for this tetrasubstituted olefin. To confirm this result, complexes **3**, **5**, and **20** were tested at a lower loading of 0.1 mol% and the reactions were monitored over time (Figure 9). At this loading, the effectiveness of the catalysts to complete the RCM dropped significantly, providing a reminder that more efficient catalysts still need to be developed.

Complex **3** outperformed both the more stable **20** and the more active **5**. At low catalyst loadings, the decreased stability of **5** becomes a larger factor than its increased activity. Complex **20** faces the opposite challenge of substantially decreased activity. The differences between **3**, **5**, and **20** suggest that increased activity becomes more important than, but does not negate, increased stability for the RCM of very challenging substrates. While conversions were low, the experiment gives a clear result and is a reminder that the key to catalyst efficiency is the ratio of the rate of productive olefin metathesis relative to the rate of catalyst decomposition.

## Conclusions

In summary, we describe the synthesis and characterization of a series of ruthenium-based olefin metathesis catalysts bearing NHCs with varying degrees of backbone and aryl substitution. In order to study their subtle differences in activity and stability, a highly sensitive assay was developed to operate at the lower limit of productive catalyst loading. These

techniques were developed using a Symyx robotic system to maintain a high degree of precision and consistency when working with ultra-low catalyst loadings.

The development of this highly sensitive assay has provided increased insight into the relationship between ligand architecture and efficiency. In this study, both backbone and aryl substitution were found to significantly impact catalyst stability and activity. Whereas low *N*-aryl bulk on the NHC ligands led to increased activity, it also decreased stability. Increased backbone substitution, however, led to increased catalyst lifetimes and decreased reaction rates. Furthermore, it was found that the relative importance of stability and activity on efficiency is dependent on the steric encumbrance of the RCM reaction. For substrates with low steric demands, catalyst stability is quite important for success at low catalyst loadings. For sterically encumbered substrates, catalyst activity becomes much more important than increased stability. The ability to study the relationship between small changes in ligand architecture and efficiency will allow us to better explore new opportunities in catalyst design.

## Experimental

### General Information

NMR spectra were recorded using a Varian Mercury 300 or Varian Inova 500 MHz spectrometer. NMR chemical shifts are reported in parts per million (ppm) downfield from tetramethylsilane (TMS) with reference to internal solvent for $^{1}H$ and $^{13}C$. Spectra are reported as follows: chemical shift (δ ppm), multiplicity, coupling constant (Hz), and integration. IR spectra were recorded on a Perkin-Elmer Paragon 1000 Spectrophotometer. Gas chromatography data was obtained using an Agilent 6850 FID gas chromatograph equipped with a DB-Wax Polyethylene Glycol capillary column (J&W Scientific). High-resolution mass spectroscopy (FAB) was completed at the California Institute of Technology Mass Spectrometry Facility. X-ray crystallographic structures were obtained by the Beckman Institute X-ray Crystallography Laboratory of the California Institute of Technology. Crystallographic data have been deposited at the CCDC, 12 Union Road, Cambridge CB2 1EZ, U.K., and copies can be obtained on request, free of charge, by quoting the publication citation and the deposition numbers 670930 (**17**) and 651007 (**20**).

All reactions involving metal complexes were conducted in oven-dried glassware under a nitrogen atmosphere with anhydrous and degassed solvents, using standard Schlenk and glovebox techniques. Anhydrous solvents were obtained via elution through a solvent column drying system.[22] Silica gel used for the purification of organometallic complexes was obtained from TSI Scientific, Cambridge, MA (60 Å, pH 6.5–7.0). $RuCl_2(PCy_3)(=CH–o\text{-}OiPrC_6H_4)$, **2**, and **3** were obtained from Materia, Inc. Unless otherwise indicated, all compounds were purchased from Aldrich or Fisher and used as obtained. The compounds **6**,[13a] **7**,[13b] **12**,[13b] **21**,[14] **24–29**,[12] have been described previously and were prepared according to literature procedures or identified by comparison of their spectroscopic data. The initial screening of the catalysts, in RCM via $^{1}H$ NMR spectroscopy was conducted according to literature procedures.[12]

### Low ppm Level Assays

Experiments on the RCM of **24**, **26**, and **28** using the catalysts described were conducted using a SymyxTM Technologies Core Module (Santa Clara, CA) housed in a Braun nitrogen-filled glovebox and equipped with Julabo LH45 and LH85 temperature-control units for separate positions of the robot tabletop.

For experiments where aliquots were not taken during the course of the reaction, up to 576 reactions (6×96 well plates) could be performed simultaneously in 1 mL vials by an Epoch software-based protocol as follows. To prepare catalyst stock solutions (0. 25 mM), 20 mL

glass scintillation vials were charged with catalyst (5 μmole) and diluted to 20.0 mL total volume in THF. Catalyst solutions, 6 to 800 μL depending on desired final catalyst loading, were transferred to reaction vials and solvent was removed via centrifugal evaporation. The catalysts were preheated to the desired temperature using the LH45 unit, and stirring was started. Substrates (0.1 mmol), containing dodecane (0.025 mmol) as an internal standard, were dispensed simultaneously to 4 reactions at a time using one arm of the robot equipped with a 4-needle assembly. Immediately following substrate addition, solvent was added to reach the desired reaction molarity, generally 1 M. All reactions were quenched by injection of 0.1 mL 5% v/v ethyl vinyl ether in toluene at a preprogrammed time. Samples were then analyzed by gas chromatography

Alternatively, where aliquots were taken during the course of the reaction, the entire operation was performed on 12 reactions simultaneously (4 catalyst loadings in triplicate or 2 catalysts at 3 catalyst loadings in duplicate) by an Epoch software-based protocol as follows. To prepare catalyst stock solutions (1.0 mM), 20 mL glass scintillation vials were charged with catalyst (5 μmole) and diluted to 5.0 mL total volume in toluene. Catalyst solutions, 10 to 400 μL depending on desired final catalyst loading, were transferred to glass 20 mL scintillation vials each capped with a septum having a 3 mm hole for the purpose of needle access, and were diluted to 10 mL total volume in toluene. The catalysts were preheated to 50.0 °C using the LH45 unit and stirred. Substrates (1 mmol), containing dodecane (0.25 mmol) as an internal standard, were dispensed simultaneously to 4 reactions at a time using one arm of the robot equipped with a 4-needle assembly. After the 2 minutes required for completion of the transfer, 50 μL aliquots of each reaction were withdrawn using the other robot arm and dispensed to 1.2 mL septa-covered vials containing 5% v/v ethyl vinyl ether in toluene cooled to −20 °C in two 96 well plates. The needle was flushed and washed between dispenses to prevent transfer of the quenching solution into the reaction vials. 16 timepoints were sampled at preprogrammed intervals and the exact times were recorded by the Epoch protocol. Samples were then analyzed by gas chromatography

### General procedure for the preparation of catalysts 15–20

To a solution of imidazolinium salt in toluene (or benzene) was added KHMDS, and the resulting solution was stirred at room temperature for a few minutes. $RuCl_2(PCy_3)(=CH–o\text{-}OiPrC_6H_4)$ was then added, and the mixture was stirred for the designated time and temperature (*vide infra*). After cooling to room temperature, the mixture was purified by column chromatography on TSI silica (eluent: hexane/diethyl ether = 2/1 → 1/1) to give the titled compounds as a green solid.

### $RuCl_2$(4,4-dimethyl-1,3-dimesityl-imidazolin-2-ylidene)$(=CH–o\text{-}OiPrC_6H_4)$ (15)

**6** (200 mg, 0.54 mmol), potassium hexamethyldisilazide (140 mg, 0.70 mmol), and $RuCl_2(PCy_3)(=CH–o\text{-}OiPrC_6H_4)$ (250 mg, 0.42 mmol) was reacted according to the general procedure (stirred for 2 h at 70 °C) to give the desired ruthenium complex **15** as a green powder (135 mg, 0.21 mmol, 49%).

$^1$H NMR (500 MHz, $CD_2Cl_2$, 25 °C): δ 16.46 (br s, 1H), 7.55 (ddd, J = 8.3 Hz, 2.0 Hz, 1H), 7.10 (br s, 2H), 7.05 (br s, 2H), 6.95 (dd, J = 7.5 Hz, 2.0 Hz, 1H), 6.91 (t, J = 7.5 Hz, 1H), 6.82 (d, J = 8.0 Hz, 1H), 4.86 (sept, J = 6.1 Hz, 1H), 3.93 (s, 2H), 2.50-2.25 (m, 18H), 1.47 (s, 6H), 1.21 (d, J = 6.1 Hz, 6H).

$^{13}$C NMR (125 MHz, $C_6D_6$): δ 293.3 (m), 213.3, 153.0, 146.4, 141.3, 139.0, 138.6, 130.7, 130.0, 129.3, 122.7, 122.5, 113.6, 75.4, 68.2 (br), 65.6 (br), 28.1, 21.8, 21.5, 21.4.

HRMS Calc'd for $C_{33}H_{42}Cl_2N_2ORu$: 654.1718. Found: 654.1725.

### $RuCl_2$(1,3-dimesityl-4,5-dimethyl-imidazolin-2-ylidene)(=CH–*o*-O*i*Pr$C_6H_4$) (16)

**7** (100 mg, 0.27 mmol), potassium hexamethyldisilazide (70 mg, 0.35 mmol), and $RuCl_2(PCy_3)$(=CH–*o*-O*i*Pr$C_6H_4$) (100 mg, 0.17 mmol) was reacted according to the general procedure (stirred for 2 h at 70 °C) to give the desired ruthenium complex **16** as a green powder (60 mg, 0.092 mmol, 54%).

$^1$H NMR (500 MHz, $C_6D_6$, 25 °C): δ 16.74 (s, 1H), 7.14 (dd, J = 7.5, 1.5 Hz, 1H), 7.11 (ddd, J = 7.5, 1.5 Hz, 1H), 7.00 (br s, 4H), 6.65 (dt, J = 7.5, 1.0 Hz, 1H), 6.32 (d, J = 8.0 Hz, 1H), 4.49 (sept, J = 6.1 Hz, 1H), 4.12 (s, 2H), 3.00-2.30 (br s, 12H), 2.25 (s, 6H), 1.31 (br s, 6H), 0.81 (d, J = 6.5 Hz, 6H).

$^{13}$C NMR (125 MHz, $C_6D_6$): δ 293.8, 213.4, 153.0, 146.4, 140.7, 138.7, 130.2, 129.9, 128.8, 122.8, 122.5, 113.6, 75.3, 62.4 (br), 21.8, 21.4, 13.9 (br).

HRMS Calc'd for $C_{33}H_{42}Cl_2N_2ORu$: 654.1718. Found: 654.1738.

### $RuCl_2$(1,3-dimesityl-4,4,5-trimethyl-imidazolin-2-ylidene)(=CH–*o*-O*i*Pr$C_6H_4$) (17)

**8** (200 mg, 0.46 mmol), potassium hexamethyldisilazide (120 mg, 0.60 mmol), and $RuCl_2(PCy_3)$(=CH–*o*-O*i*Pr$C_6H_4$) (200 mg, 0.33 mmol) was reacted according to the general procedure (stirred for 2.5 h at room temperature and 4 h at 60 °C) to give the desired ruthenium complex **17** as a green powder (97 mg, 0.15 mmol, 44%). Crystals suitable for X-ray crystallography were grown at room temperature by slow diffusion of pentane into a solution of **17** in benzene.

$^1$H NMR (500 MHz, $C_6D_6$, 25 °C): δ 16.65 (br s, 1H), 7.13-7.07 (m, 3H), 6.94 (br m, 3H), 6.63 (td, J = 7.6, 0.8 Hz, 1H), 6.31 (d, J = 8.0 Hz, 1H), 4.46 (sept, J = 6.1 Hz, 1H), 4.20 (br s, 1H), 2.85-2.47 (m, 12H), 2.24 (s, 3H), 2.21 (s, 3H), 1.28 (d, J = 6.1 Hz, 6H), 1.15 (br s, 3H), 0.88 (br s, 3H), 0.69 (br d, J = 6.9 Hz, 3H).

$^{13}$C NMR (125 MHz, $C_6D_6$): δ 293.8 (m), 213.4 (br), 152.9, 146.5, 140.7, 138.7, 138.6, 130.9, 130.6, 130.3, 129.4, 122.7, 122.4, 113.6, 75.3, 71.0 (br), 68.4 (br), 25.1, 23.1 (br), 21.8, 21.5, 21.4, 12.1.

HRMS Calc'd for $C_{34}H_{44}Cl_2N_2ORu$: 668.1875. Found: 668.1898.

### $RuCl_2$(1,3-ditolyl-4,4-dimethyl-imidazolin-2-ylidene)(=CH–*o*-O*i*Pr$C_6H_4$) (18)

**9** (190 mg, 0.60 mmol), potassium hexamethyldisilazide (157 mg, 0.78 mmol), and $RuCl_2(PCy_3)$(=CH–*o*-O*i*Pr$C_6H_4$) (200 mg, 0.33 mmol) was reacted according to the general procedure (stirred for 2 hours at 70 °C) to give the desired ruthenium complex **18** as a green powder (112 mg, 0.19 mmol, 57%).

$^1$H NMR (500 MHz, $CD_2Cl_2$, 25 °C): δ 16. 41 (br s, 0.40H), 16.24 (br s, 0.60H), 8.59 (br s, 1.20H), 8.59 (br s, 0.80H), 7.60-7.20 (m, 7H), 6.88-6.81 (m, 3H), 4.91 (m, 1H), 4.40-3.60 (m, 2H), 2.62-2.40 (m, 6H), 1.64-1.07 (m, 12H).

$^{13}$C NMR (125 MHz, $CD_2Cl_2$): δ 232.5, 152.2, 144.3, 141.9, 138.6, 134.3, 132.5, 131.4, 129.9, 129.5, 129.2, 128.9, 128.8, 127.6, 126.9, 122.3, 122.0, 121.8, 112.9, 74.8, 68.1, 66.6, 29.7, 27.3, 27.0, 26.9, 26.3, 24.6, 23.9, 21.5, 19.5.

HRMS Calc'd for $C_{29}H_{34}Cl_2N_2ORu$: 598.1092. Found: 598.1064.

### $RuCl_2$(1,3-ditolyl-4,5-dimethyl-imidazolin-2-ylidene)(=CH–*o*-O*i*Pr$C_6H_4$) (19)

**10** (100 mg, 0.32 mmol), potassium hexamethyldisilazide (70 mg, 0.35 mmol), and $RuCl_2(PCy_3)$(=CH–*o*-O*i*Pr$C_6H_4$) (100 mg, 0.17 mmol) was reacted according to the general procedure (stirred for 2 h at 70 °C) to give the desired ruthenium complex **19** as a green (39 mg, 0.065 mmol, 38%).

$^1$H NMR (500 MHz, $C_6D_6$, 25 °C): δ 16.64-16.41 (m, 1H), 9.00 (br s, 2H), 7.11-6.71 (m, 8H), 6.65 (m, 1H), 6.42 (t, J = 7.8 Hz, 1H), 4.57 (sept, J = 6.4 Hz, 1H), 4.29-3.55 (m, 2H), 2.65-2.25 (m, 6H),1.20-1.60 (m, 6H), 1.05-0.60 (m, 6H).

$^{13}$C NMR (125 MHz, $C_6D_6$): δ 291.7, 290.9, 232.5, 210.74, 152.8, 144.2, 140.0, 139.6, 138.6, 137.4, 132.4, 132.2, 131.5, 131.3, 130.6, 130.3, 121.9, 121.8, 113.0, 112.8, 74.4, 61.1, 61.0, 60.4, 21.7, 21.6, 13.2, 12.9.

HRMS Calc'd for $C_{29}H_{34}Cl_2N_2ORu$: 598.1092. Found: 598.1097.

### $RuCl_2$(1,3-ditolyl-4,4,5,5-tetramethyl-imidazolin-2-ylidene)(=CH–*o*-O*i*Pr$C_6H_4$) (20)

**11** (41 mg, 0.12 mmol), potassium hexamethyldisilazide (24 mg, 0.12 mmol), and $RuCl_2(PCy_3)$(=CH–*o*-O*i*Pr$C_6H_4$) (60 mg, 0.1 mmol) was reacted according to the general procedure described above to give the desired ruthenium complex **20** as a green powder as a ca. 3:1 mixture of isomers (45 mg, 0.072 mmol, 72%). Crystals suitable for X-ray crystallography were grown at room temperature by slow diffusion of pentane into a solution of **20** in benzene.

$^1$H NMR (500 MHz, $C_6D_6$, 25 °C): δ 16.64 (s, 0.75H), 16.33 (s, 0.25H), 8.89 (d, J = 7.7 Hz, 0.75H), 8.84 (d, J = 7.9 Hz, 0.25H), 7.43-7.25 (m, 4H), 7.20-7.05 (m, 4H), 6.99-6.94 (m, 1H), 6.70-6.62 (m, 1H), 6.34 (d, J = 8.3 Hz, 1H), 4.45 (sept, J = 6.1 Hz, 1H), 2.74 (s, 0.75H), 2.68 (s, 2.25H), 2.47 (s, 0.75H), 2.44 (s, 2.25H), 1.38-1.20 (m, 10H), 1.04 (s, 2H), 0.76-0.70 (m, 6H).

$^{13}$C NMR (125 MHz, $C_6D_6$): δ 214.0, 211.5, 153.1, 153.0, 145.8, 143.3, 143.2, 141.6, 140.8, 140.3, 139.8, 137.3, 136.5, 136.0, 134.7, 134.4, 132.3, 132.2, 131.9, 129.6, 129.5, 129.4, 129.1, 128.9, 127.6, 127.3, 126.9, 126.6, 122.7, 122.6, 122.6, 122.5, 113.5, 75.2, 75.1, 72.3, 71.8, 71.7, 71.4, 24.9, 24.3, 24.1, 23.9, 22.7, 22.5, 22.4, 22.2, 22.1, 22.0, 20.3, 20.1, 19.7, 19.4, 19.3.

HRMS Calc'd for $C_{31}H_{38}Cl_2N_2ORu$: 626.1405. Found: 626.1427.

## Supplementary Material

Refer to Web version on PubMed Central for supplementary material.

## Acknowledgement

We gratefully acknowledge financial support from the DOE (DE-FG02-08ER15933), the NIH (5RO1 GM31332), and the Gordon and Betty Moore Foundation. JBB would also like to thank Materia, Inc. for financial support. We thank Larry M. Henling and Dr. Michael W. Day (California Institute of Technology) for X-ray crystallographic analysis, and Materia, Inc. for a generous donation of ruthenium complexes, especially **2** and **3**.

## References

1. Grubbs, RH. Handbook of Metathesis. Weinheim, Germany: Wiley-VCH; 2003. and references cited therein. (b) Hoveyda AH, Zhugralin AR. Nature 2007;450:243–251. [PubMed: 17994091] (c) Schrodi Y, Pederson RL. Aldrichimica Acta 2007;40:45–52. (d) Nicolaou KC, Bulger PG, Sarlah D. Angew.

Chem., Int. Ed 2005;44:4490–4527. (e) Grubbs RH. Tetrahedron 2004;60:7117–7140. (f) Furstner A. Angew. Chem., Int. Ed 2000;39:3013–3043.

2. (a) Grubbs RH. J. Macromol. Sci. – Pure Applied Chem 1994;A31:1829–1833. (b) Trnka TM, Grubbs RH. Acc. Chem. Res 2001;34:18–29. [PubMed: 11170353]
3. Scholl M, Ding S, Lee CW, Grubbs RH. Org. Lett 1999;1:953–956. [PubMed: 10823227]
4. Garber SB, Kingsbury JS, Gray BL, Hoveyda AH. J. Am. Chem. Soc 2000;122:8168–8179.
5. (a) Chung CK, Grubbs RH. Org. Lett 2008;10:2693–2696. [PubMed: 18510331] (b) Berlin JM, Campbell K, Ritter T, Funk TW, Chlenov A, Grubbs RH. Org. Lett 2007;9:1339–1342. [PubMed: 17343392] (c) Stewart IC, Ung T, Pletnev AA, Berlin JM, Grubbs RH, Schrodi Y. Org. Lett 2007;9:1589–1592. [PubMed: 17378575] (d) Vougioukalakis GC, Grubbs RH. J. Am. Chem. Soc 2008;130:2234–2245. [PubMed: 18220390] (e) Vehlow K, Maechling S, Blechert S. Organometallics 2006;25:25–28. (f) Despagnet-Ayoub E, Grubbs RH. Organometallics 2005;24:338–340. (g) Van Veldhuizen JJ, Garber SB, Kinsgbury JS, Hoveyda AH. J. Am. Chem. Soc 2002;124:4954–4955. [PubMed: 11982348] (h) Funk TW, Berlin JM, Grubbs RH. J. Am. Chem. Soc 2006;128:1840–1846. [PubMed: 16464082] (i) Anderson DR, Lavallo V, O'Leary DJ, Bertrand G, Grubbs RH. Angew. Chem., Int. Ed 2007;46:7262–7265. (j) Kuhn KM, Grubbs RH. Org. Lett 2008;10:2075–2077. [PubMed: 18412354] (k) Weigl K, Köhler K, Dechert S, Meyer F. Organometallics 2005;24:4049–4405.
6. For recent examples, see: (a)Enquist JE, Stoltz BM. Nature 2008;453:1228–1231.1231 [PubMed: 18580947] (b)White DE, Stewart IC, Grubbs RH, Stoltz BM. J. Am. Chem. Soc 2008;130:810–811.811 [PubMed: 18163634] (c)Pfeiffer MWB, Phillips AJ. J. Am. Chem. Soc 2005;127:5334–5335.5335 [PubMed: 15826167] (d)Humphrey JM, Liao A, Rein T, Wong Y-L, Chen H-J, Courtney AK, Martin SF. J. Am. Chem. Soc 2002;124:8584–8592.8592 [PubMed: 12121099] (e)Martin SF, Humphrey JM, Ali A, Hillier MC. J. Am. Chem. Soc 1999;121:866–867.867 (f)Yang Z, He Y, Vourloumis D, Vallberg H, Nicolaou KC. Angew. Chem., Int. Ed 1997;36:166–168.168
7. (a) Maynard HD, Grubbs RH. Tetrahedron Lett 1999;40:4137–4140. (b) Hong SH, Sanders DP, Lee CW, Grubbs RH. J. Am. Chem. Soc 2005;127:17160–17161. [PubMed: 16332044]
8. Governmental recommendations for residual ruthenium are now routinely less than 10 ppm. For recent guidelines, see: Zaidi K. Pharmacopeial Forum 2008;34:1345–1348.1348 (b) Criteria given in the EMEA Guideline on the Specification Limits for Residues of Metal Catalysts, available at: http://www.emea.europa.eu/pdfs/human/swp/444600.pdf
9. (a) Ulman M, Grubbs RH. J. Org. Chem 1999;64:7202–7207. (b) Hong SH, Day MW, Grubbs RH. J. Am. Chem. Soc 2004;126:7414–7415. [PubMed: 15198568] (c) Hong SH, Wenzel AG, Salguero TT, Day MW, Grubbs RH. J. Am. Chem. Soc 2007;129:7961–7968. [PubMed: 17547403] (d) Hong SH, Chlenov A, Day MW, Grubbs RH. Angew. Chem., Int. Ed 2007;46:5148–5151. (e) Vehlow K, Gessler S, Blechert S. Angew. Chem., Int. Ed 2007;46:8082–8085. (f) Leitao EM, Dubberley SR, Piers WE, Wu Q, McDonald R. Chem. Eur. J 2008;14:11565–11572.
10. Under inert atmosphere, heating a $C_6D_6$ solution of catalyst **5** for 3 days at 70 ° leads to its total decomposition, while catalyst **2** doesn't readily decompose under those conditions.
11. Occhipinti G, Bjorsvik H-R, Jensen VR. J. Am. Chem. Soc 2006;128:6952–6964. [PubMed: 16719476]
12. Ritter T, Hejl A, Wenzel AG, Funk TW, Grubbs RH. Organometallics 2006;25:5740–5745.and literature cited therein.
13. (a) Jazzar R, Bourg J-B, Dewhurst RD, Donnadieu B, Bertrand G. J. Org. Chem 2007;72:3492–3499. [PubMed: 17408289] (b) Türkmen H, Çetinkaya B. J. Organomet. Chem 2006;691:3749–3759.
14. Denk K, Sirsch P, Herrmann WA. J. Organomet. Chem 2002;649:219–224.
15. In this paper, catalyst activity encompasses initiation and propagation rates. For more insight into initiation kinetic studies, see Sanford MS, Love JA, Grubbs RH. J. Am. Chem. Soc 2001;123:6543–6554.6554 [PubMed: 11439041]
16. Catalyst stability refers to the ability of a catalyst to do productive metathesis after extended period of time.
17. Champagne, TM.; Hong, SH.; Lee, CW.; Ung, TA.; Stoianova, DS.; Pederson, RL.; Kuhn, KM.; Virgil, SC.; Grubbs, RH. Abstracts of Papers; 236th ACS National Meeting; Philadelphia, PA.

Washington, DC: American Chemical Society; 2008. ORGN-077 (b) Matson JM, Virgil SC, Grubbs RH. J. Am. Chem. Soc. in press

18. Bieniek M, Michrowska A, Usanov DL, Grela K. Chem Eur. J 2008;14:806–818.
19. Ethyl vinyl ether functions as an effective catalyst quench, as the corresponding Fischer carbene complex is metathesis inactive. See: Louie J, Grubbs RH. Organometallics 2002;21:2153–2164.2164
20. Wang H, Goodman SN, Dai Q, Stockdale GW, Clark WM Jr. Org. Process Res. Dev 2008;12:226–234.
21. Complexes **15**, **16**, **18** and **19** underwent no further testing as experimentation continually demonstrated that complexes bearing disubstituted backbone ligands consistently gave results between the two extremes.
22. Pangborn AB, Giardello MA, Grubbs RH, Rosen RK, Timmers FJ. Organometallics 1996;15:1518–1520.

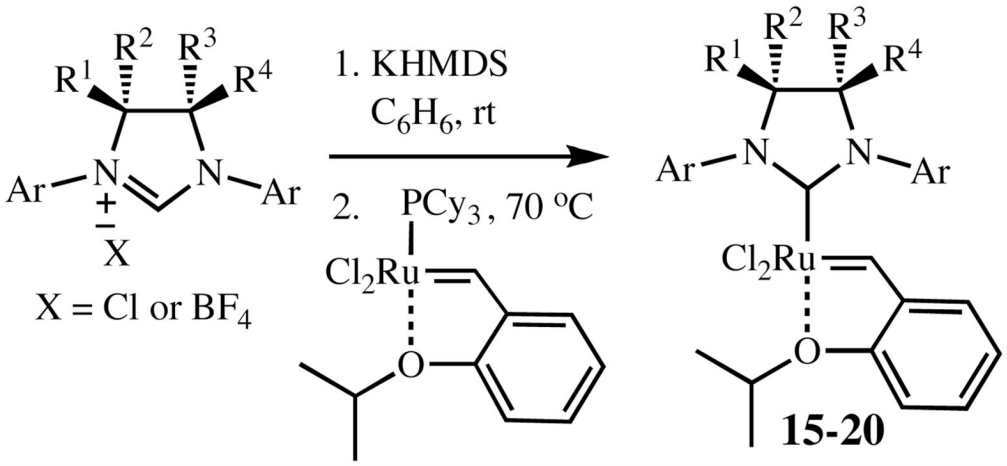


| | Ar | $R^1$ | $R^2$ | $R^3$ | $R^4$ | % Yield |
|---|---|---|---|---|---|---|
| **15** | Mesityl | H | H | Me | Me | 49 |
| **16** | Mesityl | Me | H | H | Me | 54 |
| **17** | Mesityl | H | Me | Me | Me | 44 |
| **18** | *o*-Tolyl | H | H | Me | Me | 57 |
| **19**[a] | *o*-Tolyl | H (Me) | Me (H) | H | Me | 38 |
| **20** | *o*-Tolyl | Me | Me | Me | Me | 72 |

[a] Backbone methyl groups are a mixture of *syn*- and *anti*- isomers.

**Figure 1.**
Synthesis of ruthenium complexes **15–20**.

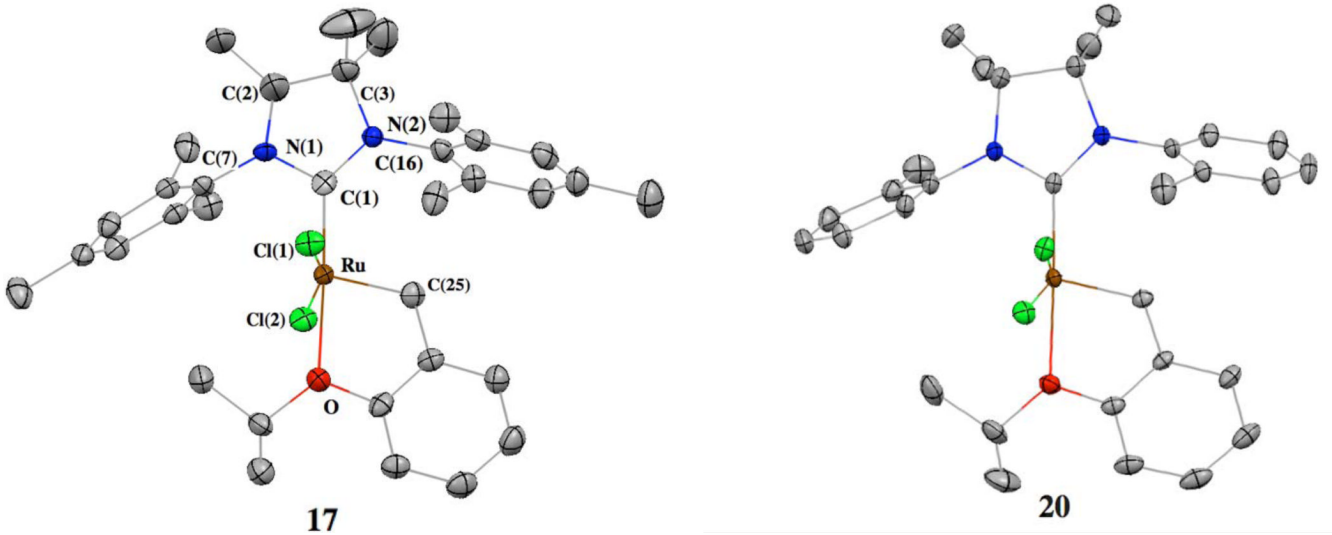


**Figure 2.**
X-ray crystal structures of complexes **17** and **20** are shown. Displacement ellipsoids are drawn at 50% probability. For clarity, hydrogen atoms have been omitted.

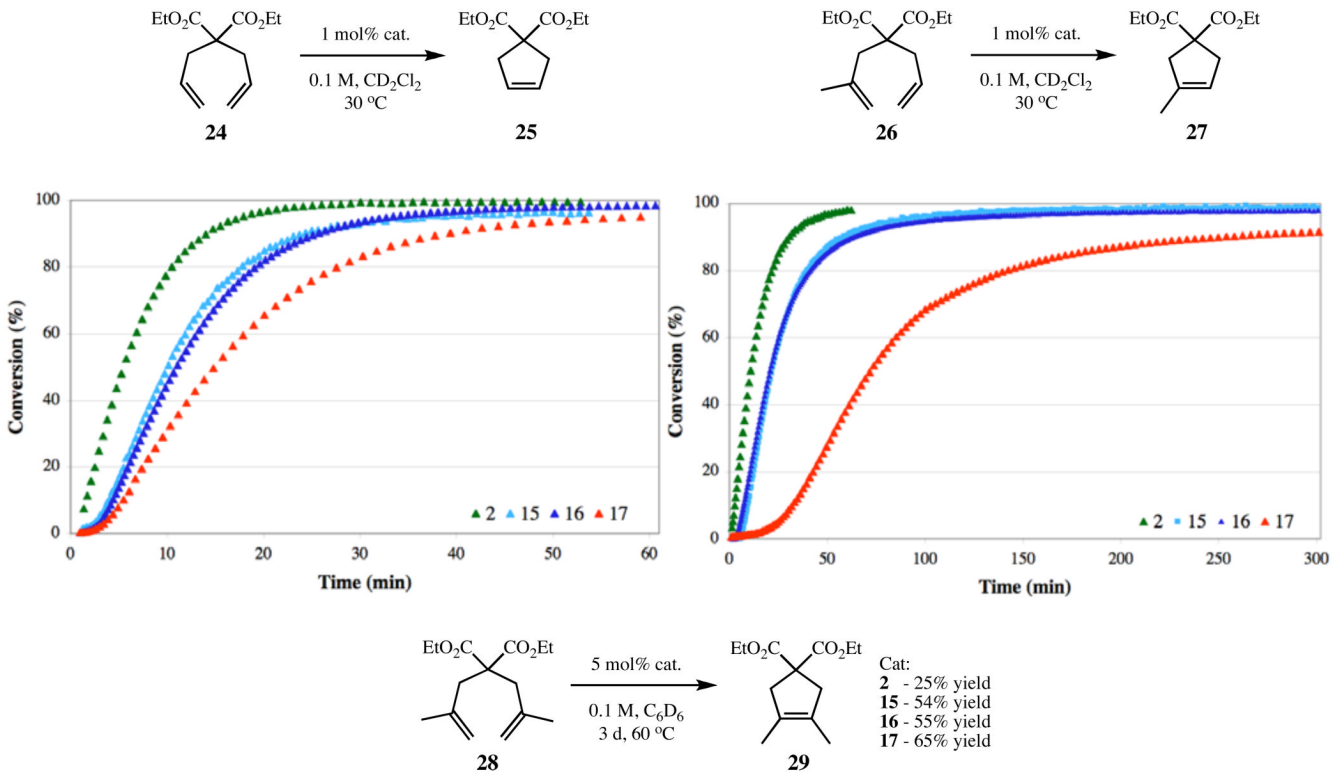


**Figure 3.**
RCM of dienes **24**, **26**, and **28** to di-, tri-, and tetrasubstituted cycloalkenes **25**, **27**, and **29**, respectively, using catalysts **2** and **15–17**.

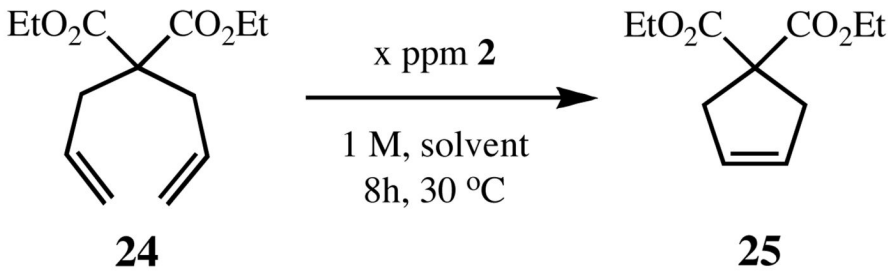


**24** **25**

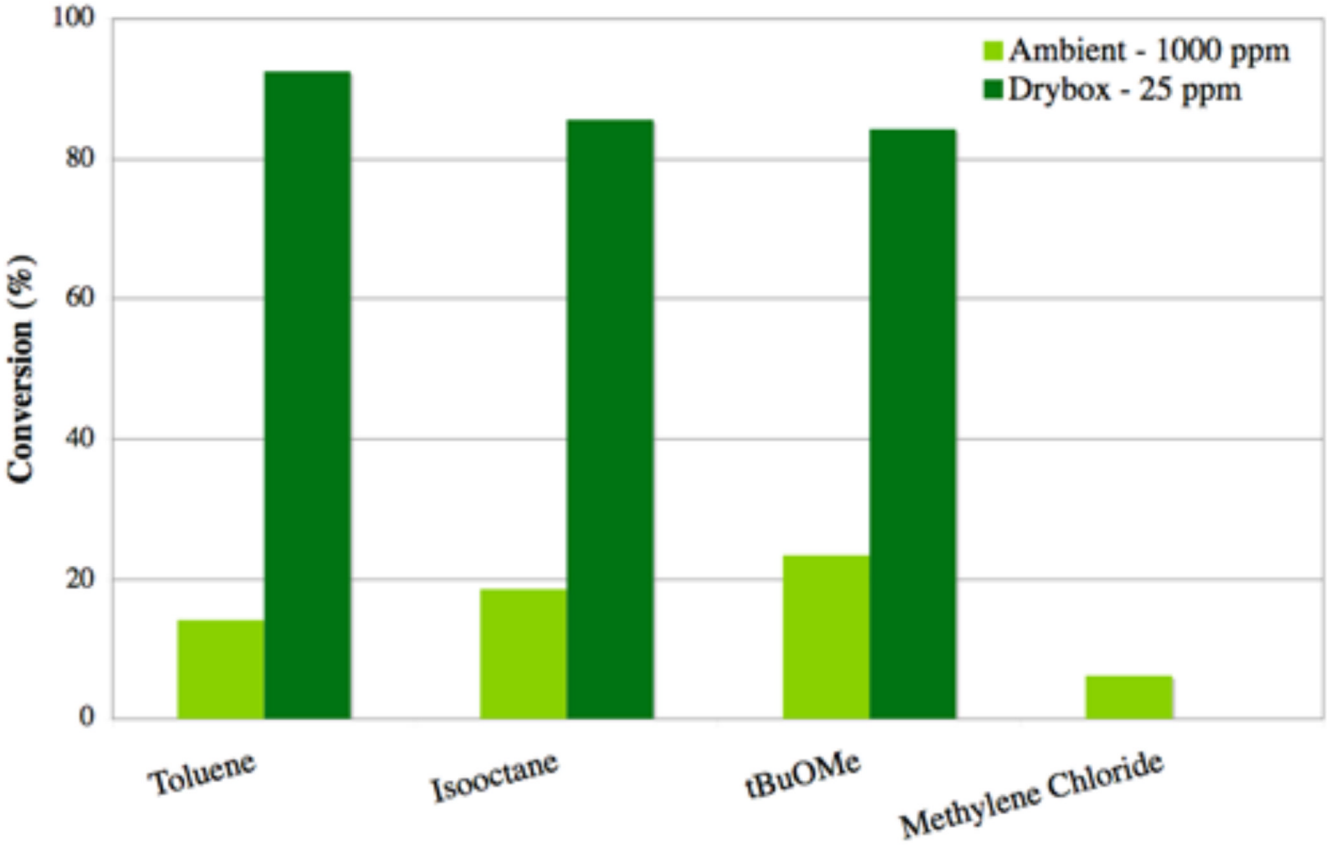


**Figure 4.**
RCM of diene **24** to disubstituted cycloalkene **25**, using catalyst **2** in a variety of solvents.

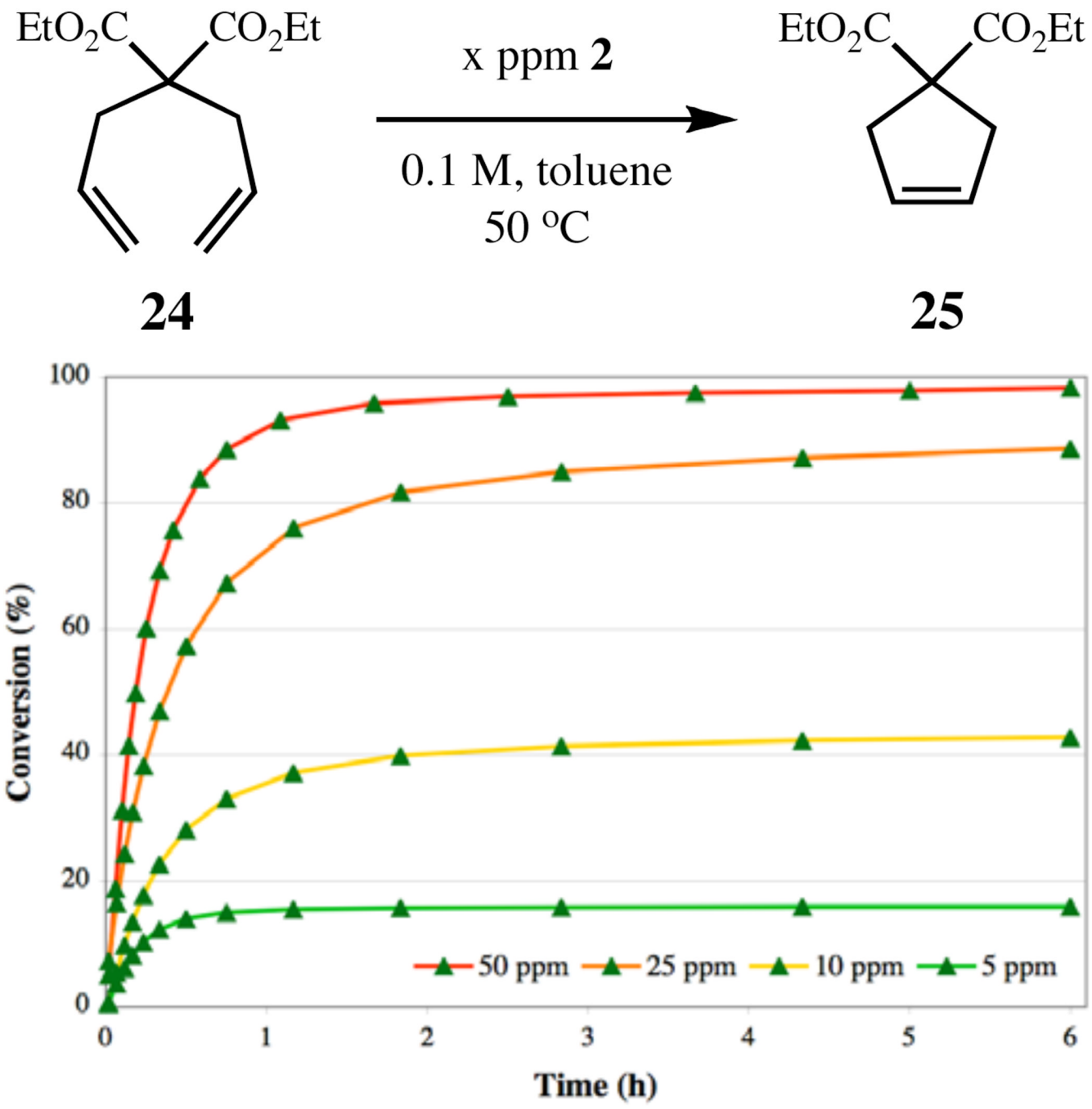


**Figure 5.**
RCM of diene **24** to disubstituted cycloalkene **25**, using catalyst **2**.

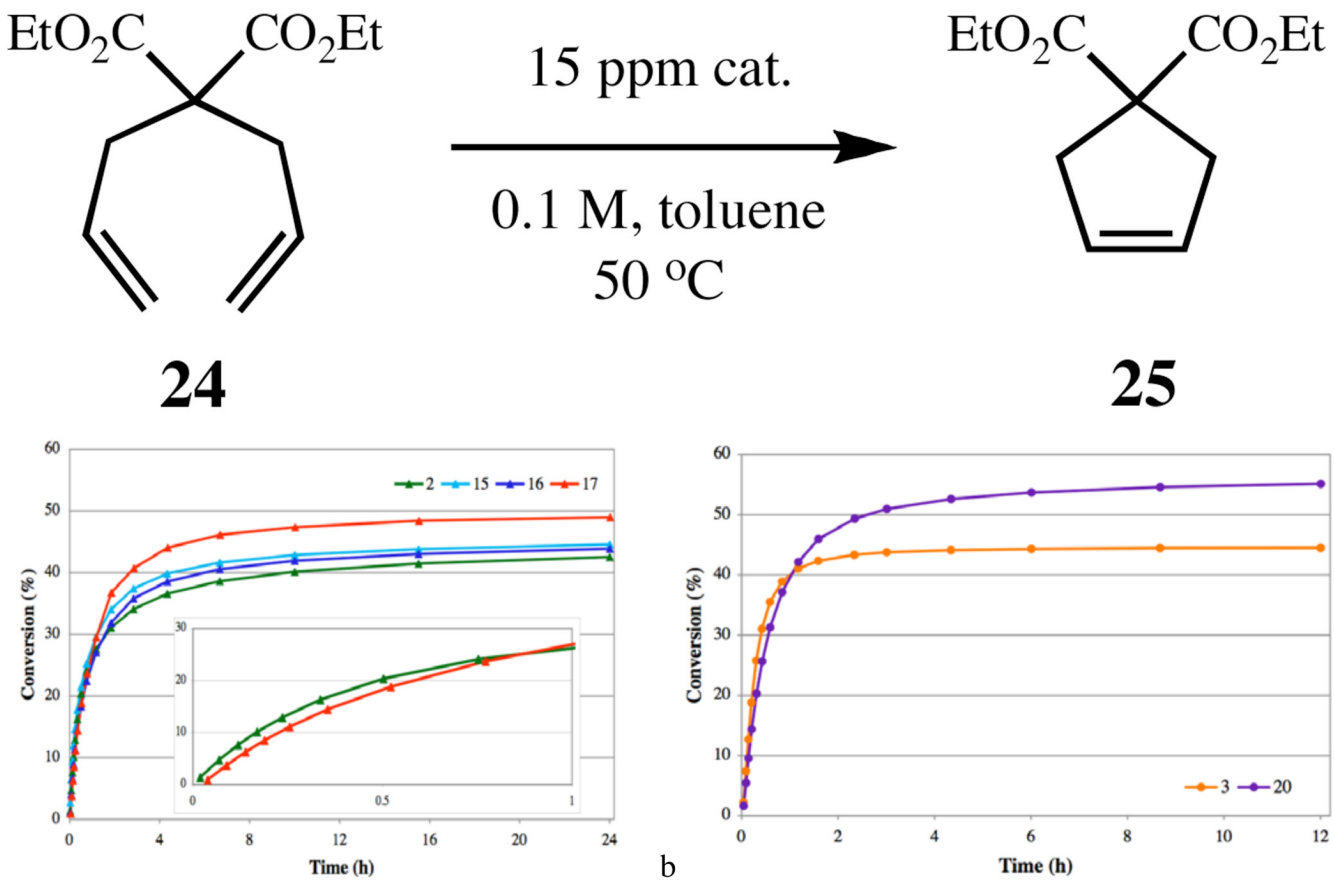


**Figure 6.**

Plot of the RCM of diene **24** to disubstituted cycloalkene **25**, with conversion monitored over 24 h: (a) Using catalysts **2** and **15–17**. The inset depicts a plot expansion over 1 h of the reaction. (b) Using catalysts **3** and **20**.

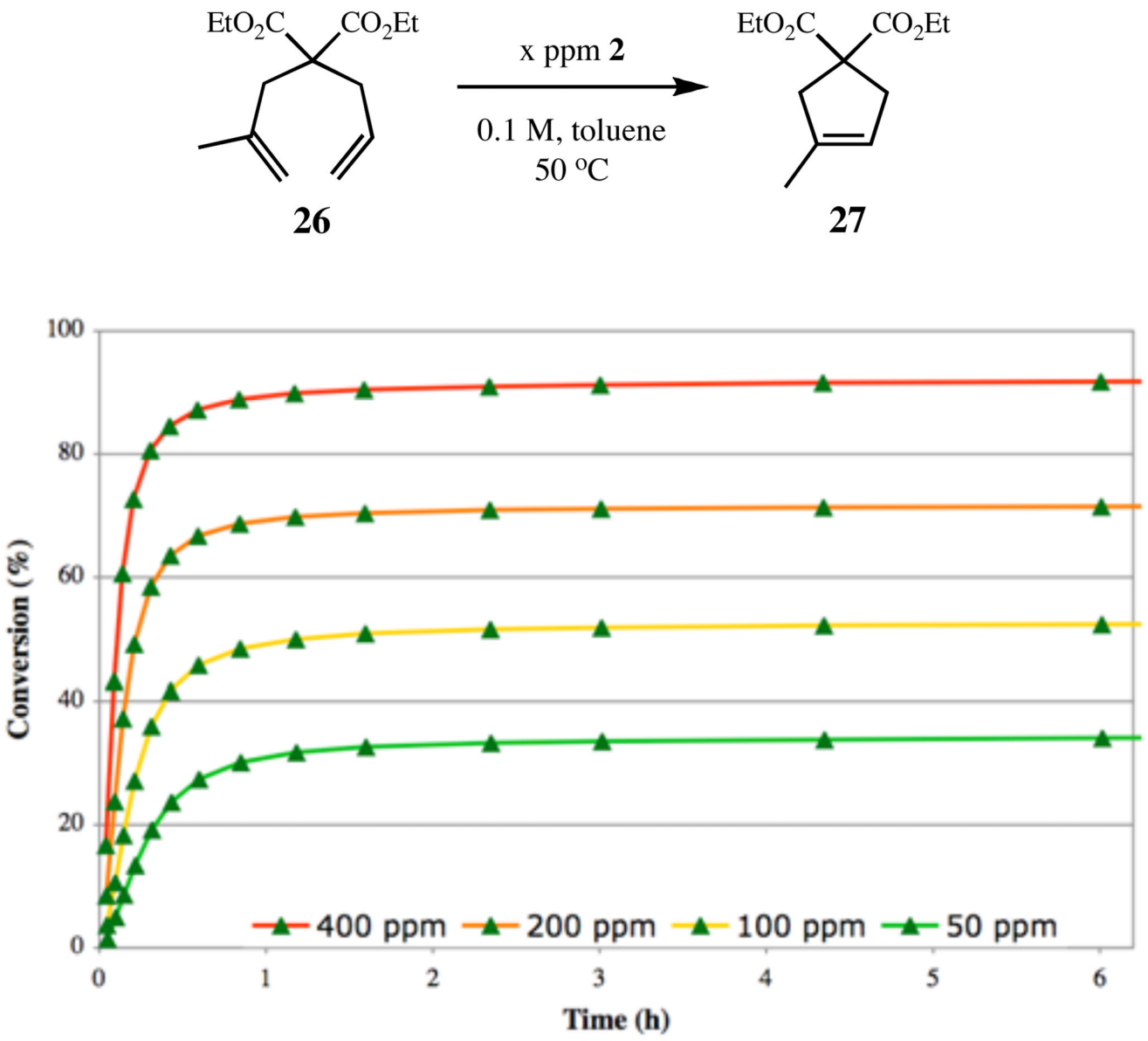


**Figure 7.**
RCM of diene **26** to disubstituted cycloalkene **27**, using catalyst **2**.

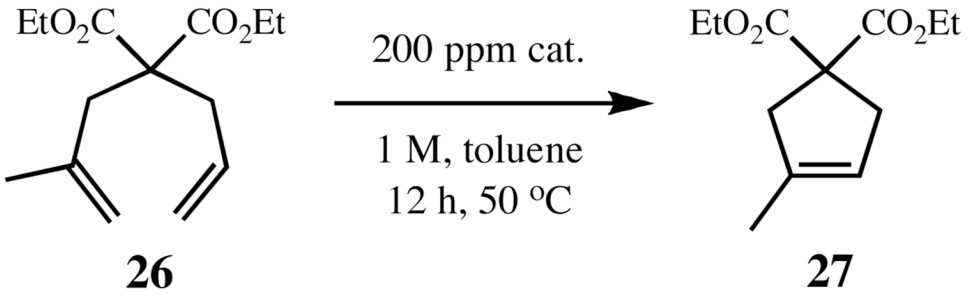


**26** **27**

| Cat. | Yield (%) |
|---|---|
| **2** | 77 |
| **17** | 84 |
| **3** | 54 |
| **20** | 64 |
| **5** | 31 |

**Figure 8.**
RCM of diene **26** to trisubstituted cycloalkene **27**, using catalysts **2**, **3**, **5**, **17**, and **20**.

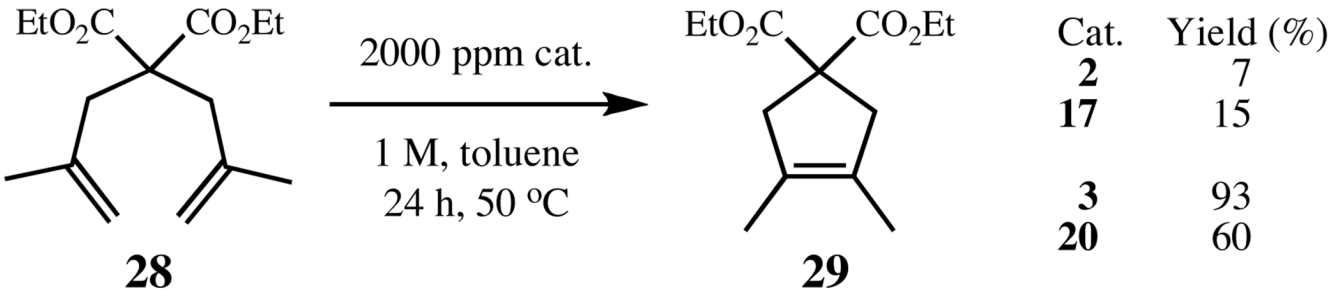


**Figure 9.**
RCM of diene **28** to tetrasubstituted cycloalkene **29**, using catalysts **2**, **3**, **17**, and **20**.

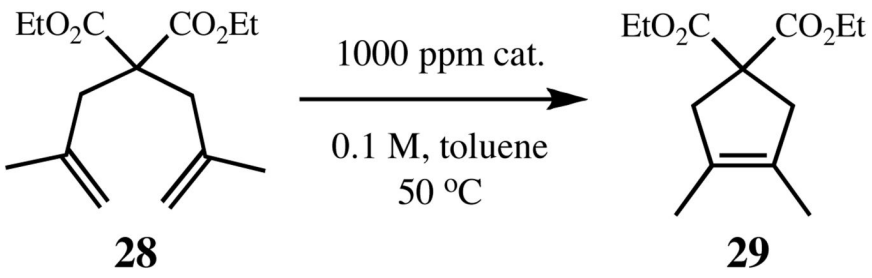


**28** **29**

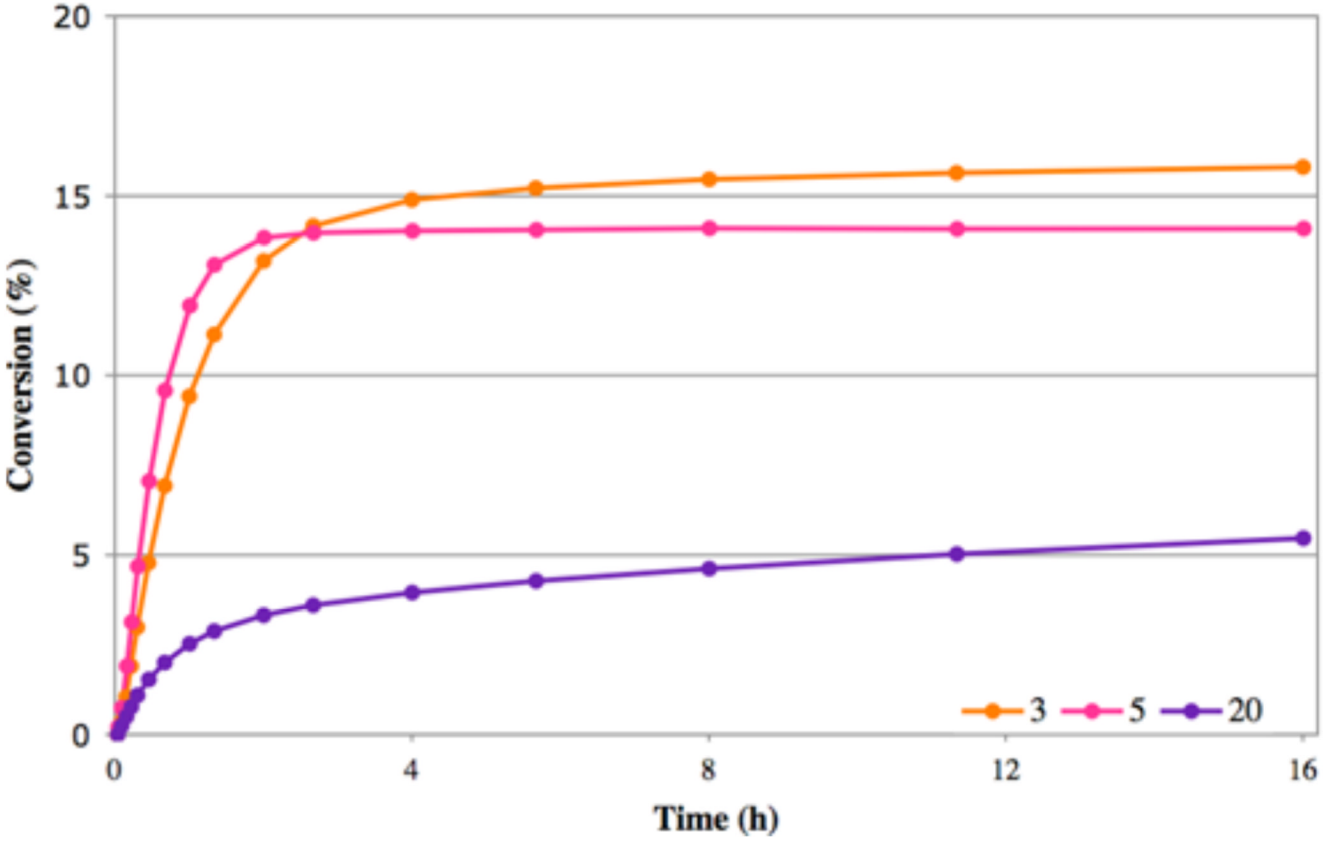


**Figure 10.**
RCM of diene **28** to tetrasubstituted cycloalkene **29**, using catalysts **3**, **5**, and **20**.

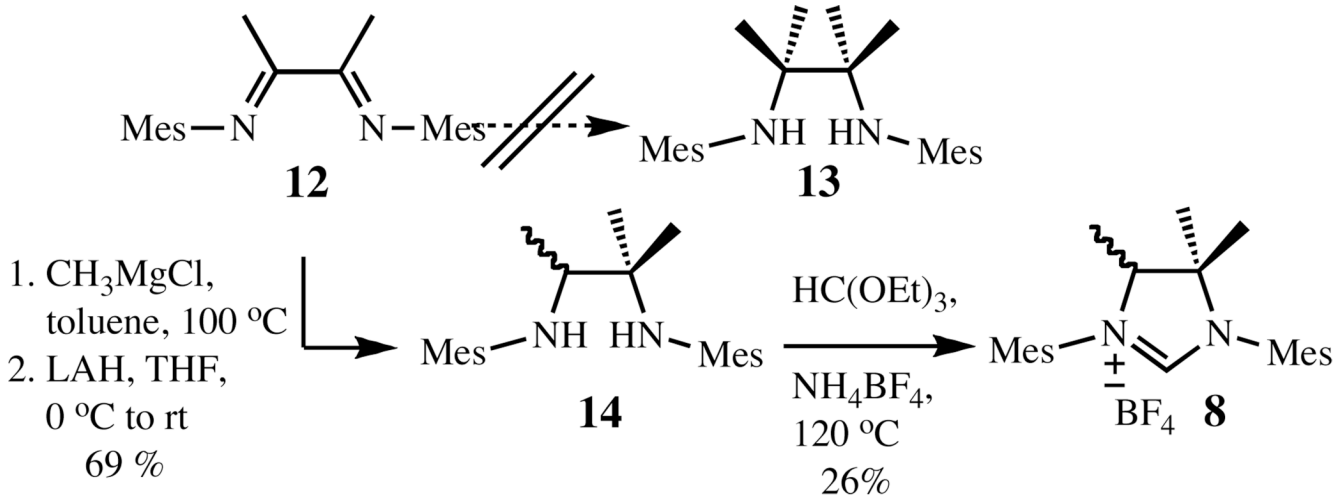


**Scheme 1.**
Synthesis of imidazolinium chloride **8**.

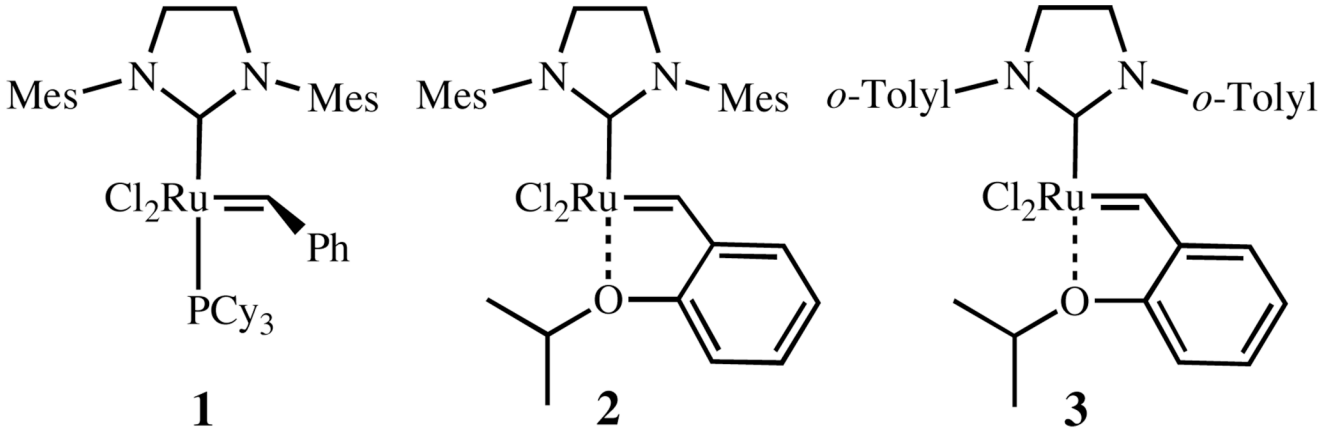


**Chart 1.**
Representative NHC-bearing olefin metathesis catalysts.

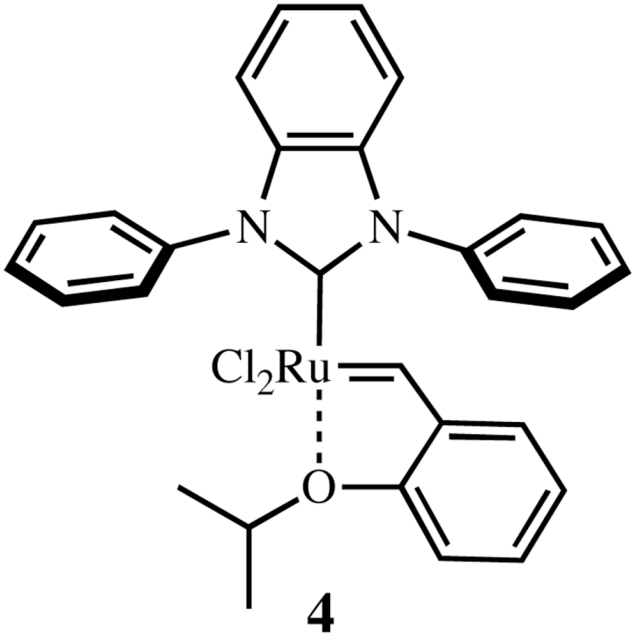


**4**

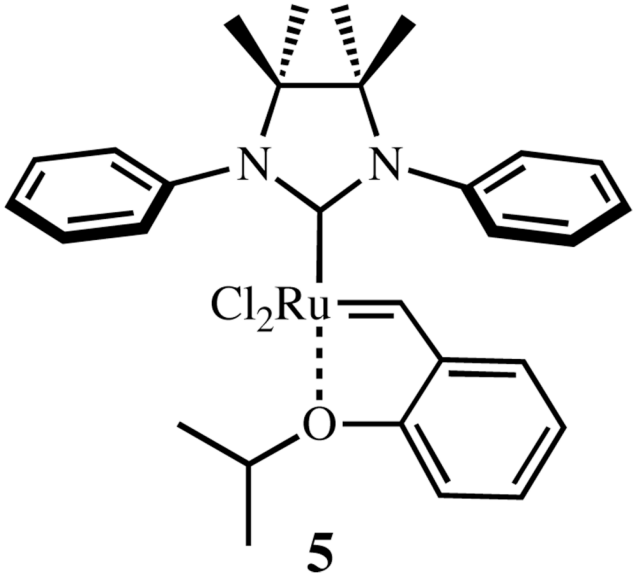


**5**

**Chart 2.**
*N*-phenyl substituted complexes.

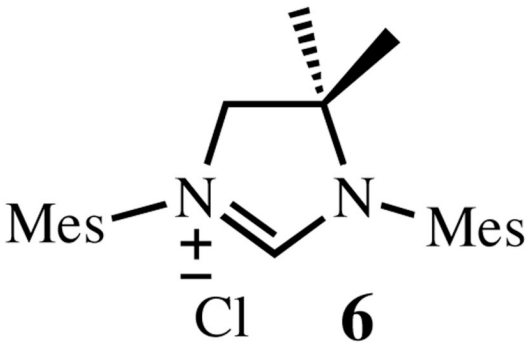


**6**

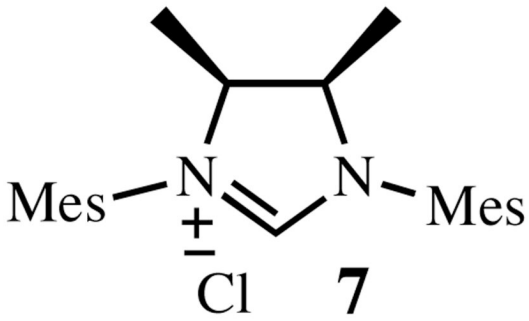


**7**

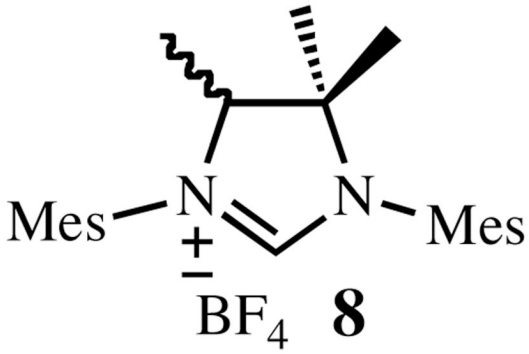


**8**

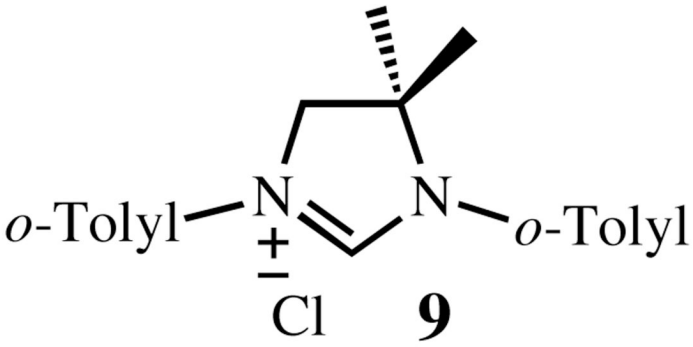


**9**

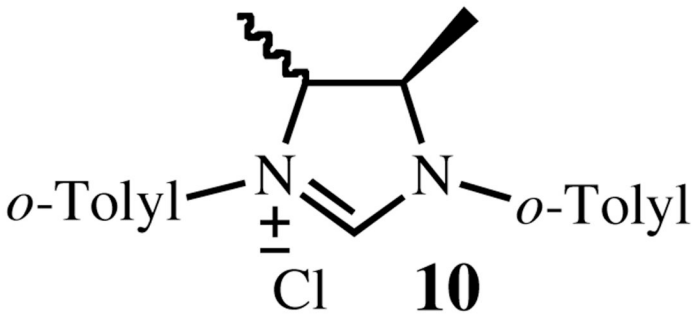


**10**

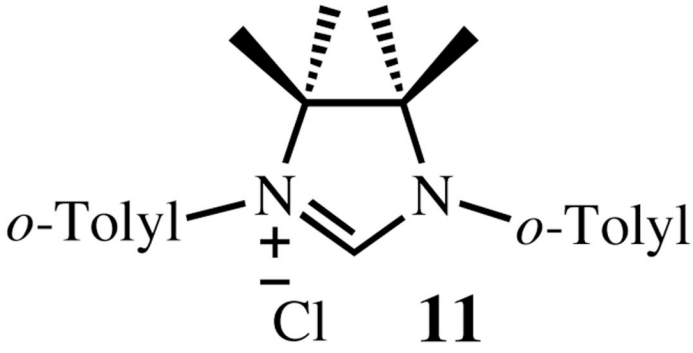


**11**

**Chart 3.**
Imidazolinium salts.

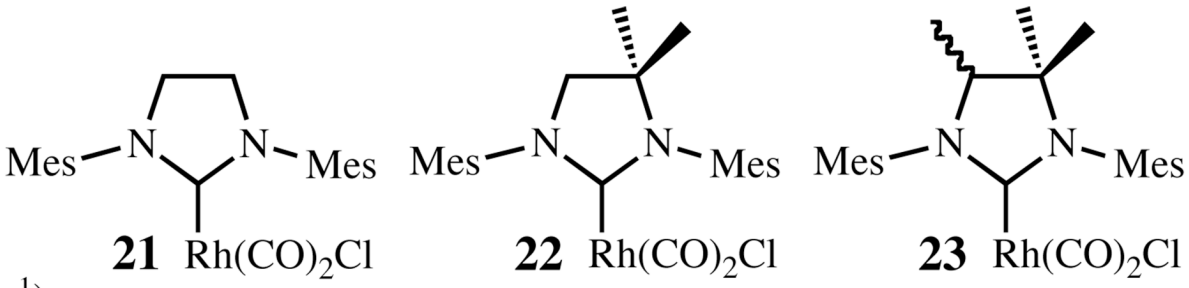


| $\nu_{CO}$ ($cm^{-1}$) | | | |
|---|---|---|---|
| sym | 2081 | 2079 | 2077 |
| asym | 1996 | 1995 | 1994 |

**Chart 15.**
IR carbonyl stretching frequencies of *cis*-[$RhCl(CO)_2$(NHC)] complexes **21–23**.

**Table 1**

Selected X-ray data for **2**, **17**, **3**, and **20**.[a]

| | **2**[b] | **17** | **3**[c] | **20** |
|---|---|---|---|---|
| **Bond Length** (Å) | | | | |
| Ru-C(1) | 1.980 | 1.968 | 1.962 | 1.964 |
| RuC(25) | 1.824 | 1.840 | 1.823 | 1.835 |
| Ru-O | 2.262 | 2.255 | 2.244 | 2.261 |
| **Bond Angles** (deg) | | | | |
| C(3)-N(2)-C(16) | 118.22 | 122.60 | 119.91 | 119.82 |
| C(2)-N(1)-C(7) | 118.32 | 123.82 | 120.69 | 120.26 |
| C(1)-Ru-C(25) | 101.42 | 103.08 | 102.48 | 103.14 |
| C(1)-Ru-Cl(2) | 156.42 | 161.26 | 159.49 | 160.80 |

[a] For a complete list of bond lengths and angles for **17** and **20**, refer to the SI.

[b] See ref 4.

[c] See ref 5c.